## Robust far-from-equilibrium spin segregation with ultracold fermionic atoms

Ulrich Ebling<sup>1</sup>, André Eckardt<sup>1</sup>,\* and Maciej Lewenstein<sup>1,2</sup>

We investigate theoretically the time evolution of spin-1/2 fermions in a harmonic trap after, initially, a spiral spin configuration far-from equilibrium is created. We predict a spin segregation building up in time already for weak interaction. The effect relies on an interplay between exchange interaction and the harmonic trap. Is is observed for a wide range of parameters.

PACS numbers: 67.10.Hk, 67.30.hj, 05.20.Dd

Keywords: Fermi gas, off-equilibrium dynamics, many-body dynamics, exchange interaction, spin segregation

Ultracold atomic quantum gases have been established as a clean and tunable test ground for many-body physics [1]. They allow to mimic condensed matter, but offer also opportunities to study aspects of many-body physics that are hard to address in other systems. An important example for the latter is the broad and widely unexplored subject of many-body dynamics. Here we investigate theoretically the far-from equilibrium dynamics of repulsively interacting spin-1/2 fermions in a one-dimensional harmonic trap. The initial state is created out of the spinpolarized equilibrium by rotating the spins spatially into a spiral configuration (as previously done for a Bose condensate [2] and proposed for strongly interacting fermions for the purpose of probing the Stoner transition[3]). We show that already weak interaction, like in the experiment described in Refs. [4, 5], is sufficient to induce a robust spin segregation in the course of time. This finding stands in contrast to the equilibrium physics of the system that is not affected much by weak interaction. For example the spin segregation of itinerant ferromagnetism (recently observed indirectly in a cold-atom system [6]) requires strong repulsion (as well as higher dimensions). The experiment [6] has inspired also theoretical work on the dynamics of strongly-interacting spin-1/2 fermions, e.g. Refs. [3, 7]; we study dynamics for weak interaction.

We consider a gas of fermionic atoms of mass M having two relevant internal states,  $m=\frac{1}{2},-\frac{1}{2}\equiv\uparrow,\downarrow$ . The gas is not necessarily quantum degenerate but sufficiently cold and dilute to interact via low-energy s-wave scattering only. Consequently, the interaction between two particles 1 and 2 is captured by a pseudo potential  $U'_{m'_1m_1,m'_2m_2}\delta(\mathbf{r}_1-\mathbf{r}_2)$  with  $(m_1,m_2)$  and  $(m'_1,m'_2)$  denoting the spin state before and after scattering, respectively. Since s-wave scattering requires the relative spin state to be the antisymmetric singlet, one has  $U'_{m'_1m_1,m'_2m_2}=g'P_{m'_1m_1,m'_2m_2}$  with

$$P_{m'_{1}m_{1},m'_{2}m_{2}} = (e_{m'_{1}m_{1}}e_{m'_{2}m_{2}} - e_{m'_{2}m_{1}}e_{m'_{1}m_{2}})/2$$

$$= e_{m'_{1}m_{1}}e_{m'_{2}m_{2}}/4 - \mathbf{s}_{m'_{1}m_{1}} \cdot \mathbf{s}_{m'_{2}m_{2}}. (1)$$

projecting on the singlet state. Here  $e_{m'm}$  and  $s_{m'm}$  are the unity matrix and the vector of spin-1/2 matri-

ces. The term  $-e_{m'_2m_1}e_{m'_1m_2}/2$  corresponds to the exchange interaction and gives rise to the spin-spin coupling  $-\mathbf{s}_{m_1'm_1}\cdot\mathbf{s}_{m_2'm_2}$ . The coupling constant  $g'=4\pi\hbar^2a_s/M$ is proportional to the singlet s-wave scattering length  $a_s$ , characterizing the actual interatomic potential. The Hamiltonian reads  $\hat{H}' = \int d\mathbf{r} \, \hat{\psi}^{\dagger}_{m'}(\mathbf{r}) h'_{m'm}(\mathbf{r}) \hat{\psi}_{m}(\mathbf{r}) +$  $\frac{g'}{2} \int d\mathbf{r} \, \hat{\psi}_{m'_1}^{\dagger}(\mathbf{r}) \hat{\psi}_{m'_2}^{\dagger}(\mathbf{r}) P_{m'_1 m_1, m'_2 m_2} \hat{\psi}_{m_2}(\mathbf{r}) \hat{\psi}_{m_1}(\mathbf{r}).$ peated spin indices imply summation,  $\hat{\psi}_m(\mathbf{r})$  is a field operator,  $h'_{m'm}(\mathbf{r}) = -\frac{\hbar^2}{2M} \nabla^2_{\mathbf{r}} e_{m'm} + V'_{m'm}(\mathbf{r})$  denotes the single-particle Hamiltonian, and  $V'_{m'm}(\mathbf{r}) = V(\mathbf{r}) e_{m'm} +$  $m{B}(m{r}) \cdot m{s}_{m'm}$  describes a spin-sensitive optically or magnetically created potential, decomposed into a scalar part V'(r) and an effective magnetic field B(r). We consider a harmonic confining potential  $V'(r) \equiv V(x) + V_{\perp}(y,z) =$  $\frac{1}{2}M[\omega^2x^2+\omega_{\perp}^2(y^2+z^2)]$  and that the magnetic field varies in x-direction only, B(r) = B(x). We assume, moreover, a tight transversal confinement, with  $\hbar\omega_{\perp}$  larger than temperature or chemical potential, such that the particles basically occupy the transversal single-particle ground state. Introducing a dimensionless description in units of the longitudinal trap [energies, lengths, momenta, and times are given from now on in multiples of  $\hbar\omega$ ,  $(M\omega/\hbar)^{-1/2}$ ,  $(M\hbar\omega)^{1/2}$ , and  $\omega^{-1}$ , respectively] we arrive at the 1D Hamiltonian

$$\hat{H} = \int \mathrm{d}x \,\hat{\psi}_{m'}^{\dagger}(x) h_{m'm}(x) \hat{\psi}_m(x) \tag{2}$$

$$+\frac{g}{2}\int \mathrm{d}x\,\hat{\psi}^{\dagger}_{m'_{1}}(x)\hat{\psi}^{\dagger}_{m'_{2}}(x)P_{m'_{1}m_{1},m'_{2}m_{2}}\hat{\psi}_{m_{2}}(x)\hat{\psi}_{m_{1}}(x)$$

with  $g=2\hbar\omega_{\perp}a_s\times(M\omega/\hbar)^{1/2}/(\hbar\omega),\ h_{m'm}(x)=-\frac{1}{2}\partial_x^2e_{m'm}+V_{m'm}(x),\ \text{and}\ V_{m'm}(x)=\frac{1}{2}x^2e_{m'm}+B(x)\cdot s_{m'm}.$  The interaction can be simplified to  $\hat{H}_{\mathrm{int}}=g\int \mathrm{d}x\,\hat{\psi}_{\uparrow}^{\dagger}(x)\hat{\psi}_{\downarrow}^{\dagger}(x)\hat{\psi}_{\downarrow}(x)\hat{\psi}_{\uparrow}(x)$  making explicit that by Pauli exclusion only fermions of opposite spin interact. The resulting spin coupling – repulsion is avoided by parallel spin orientation – is more apparent, however, in Eqs. (1) and (2), which inherit already the antisymmetry with respect to particle exchange.

We study the system's dynamics in terms of the singleparticle density matrix  $n_{m'm}(x',x) \equiv \langle \hat{\psi}_{m'}^{\dagger}(x')\hat{\psi}_{m}(x)\rangle$ , obeying  $i\dot{n}_{m'm}(x',x) = \langle [\hat{\psi}_{m'}^{\dagger}(x')\hat{\psi}_{m}(x),\hat{H}]\rangle$ . While for

<sup>&</sup>lt;sup>1</sup>ICFO-Institut de Ciències Fotòniques, Av. Canal Olímpic s/n, E-08860 Castelldefels (Barcelona), Spain, and <sup>2</sup>ICREA-Institucio Catalana de Recerca i Estudis Avançats, Lluis Companys 23, E-08010 Barcelona, Spain (Dated: April 09, 2011)

non-interacting particles the r.h.s. of this equation reads  $h_{mk}(x)n_{m'k}(x',x) - h_{km'}(x)n_{km}(x',x)$ , the interaction  $\hat{H}_{\rm int}$  leads to quartic expectation values that we decompose like  $\langle \hat{\psi}_k^{\dagger} \hat{\psi}_l^{\dagger} \hat{\psi}_m \hat{\psi}_n \rangle \approx \langle \hat{\psi}_k^{\dagger} \hat{\psi}_n \rangle \langle \hat{\psi}_l^{\dagger} \hat{\psi}_m \rangle - \langle \hat{\psi}_k^{\dagger} \hat{\psi}_m \rangle \langle \hat{\psi}_l^{\dagger} \hat{\psi}_n \rangle$  in order to get a closed equation for  $n_{m'm}(x',x)$ . By Wick's theorem this decomposition is exact for the initial state considered here, being an equilibrium state of a quadratic Hamiltonian modified only by the spiral spin rotation generated by another quadratic Hamiltonian. At later times it corresponds to the time-dependent Hartree-Fock approximation that is suitable for weak interaction and leads to the non-linear equation of motion

$$i\dot{n}_{m'm}(x',x) = h_{mk}^{\rm mf}(x)n_{m'k}(x',x) - h_{km'}^{\rm mf}(x')n_{km}(x',x).$$
(3)

Here  $h_{m'm}^{\text{mf}}(x) = h_{m'm}(x) + V_{m'm}^{\text{mf}}(x)$  plays the role of a single-particle Hamiltonian and comprises the mean-field potential  $V_{m'm}^{\text{mf}}(x) = V^{\text{mf}}(x)e_{m'm} + \boldsymbol{B}^{\text{mf}}(x) \cdot \boldsymbol{s}_{m'm}$  where

$$V_{\rm mf}(x) = g n_0(x)/2, \qquad \boldsymbol{B}_{\rm mf}(x) = -2g \boldsymbol{n}(x), \quad (4$$

with particle density  $n_0(x) = e_{m'm} n_{m'm}(x, x)$  and spin density  $\mathbf{n}(x) = \mathbf{s}_{m'm} n_{m'm}(x, x)$ . The mean-field potential (4) inherits the structure of the projector (1).

As a final step, we introduce the Wigner function

$$w_{m'm}(x,p) = \frac{1}{2\pi} \int d\xi \, e^{-ip\xi} n_{m'm}(x-\xi/2, x+\xi/2).$$
 (5)

Using Eq. (3), this phase-space representation of the single-particle density matrix is shown to evolve like

$$\dot{w}_{m'm}(x,p) = -p\partial_x w_{m'm}(x,p) + \frac{1}{i} \sum_{\alpha=0}^{\infty} \frac{1}{\alpha!} \left(\frac{i}{2} \partial_y \partial_p\right)^{\alpha}$$

$$\times [\bar{V}_{mk}(y)w_{m'k}(x,p) - (-)^{\alpha}\bar{V}_{km'}(y)w_{km}(x,p)]\Big|_{y=x}$$
 (6)

with  $\bar{V}_{m'm}(x) \equiv V_{m'm}(x) + V_{m'm}^{\text{mf}}(x); n_{m'm}(x,x) =$  $\int dp \, w_{m'm}(x,p)$  closes this equation of motion. We employ a semiclassical approximation to the *motional* degrees of freedom by truncating the infinite series after  $\alpha = 1$ . This is justified as long as the potential  $\bar{V}_{m'm}(x)$  varies slowly compared to the single-particle wave lengths involved. It is, thus, particularly suitable for sufficiently hot or dense systems, with either the thermal or the Fermi wave length small. Moreover, the truncation is exact for harmonic or linear potentials  $\bar{V}_{m'm}(x)$ . It gives  $\dot{w}_{m'm} = -p\partial_x w_{m'm} + (\partial_x \bar{V})\partial_p w_{m'm} - i\bar{B}$ .  $(s_{mk}w_{m'k}-s_{km'}w_{km})+\frac{1}{2}(\partial_x\bar{B})\cdot\partial_p(s_{mk}w_{m'k}+s_{km'}w_{km})$ having the form of a Boltzmann equation, lacking the collision integral and augmented by a coherent spindynamics [8]. On the r.h.s., the four terms describe diffusion, spin-independent acceleration, coherent spin rotation, and spin-dependent acceleration, respectively. It is instructive to introduce the real-valued density and spin Wigner functions  $w_0(x,p) \equiv e_{m'm} w_{m'm}(x,p)$  and  $\boldsymbol{w}(x,p) \equiv \boldsymbol{s}_{m'm} w_{m'm}(x,p)$ . They follow

$$\dot{w}_{0} = \left(-p\partial_{x} + (\partial_{x}\bar{V})\partial_{p}\right)w_{0} + (\partial_{x}\bar{\boldsymbol{B}})\cdot\partial_{p}\boldsymbol{w}, \tag{7}$$

$$\dot{\boldsymbol{w}} = \left(-p\partial_{x} + (\partial_{x}\bar{V})\partial_{p} + \bar{\boldsymbol{B}}\times\right)\boldsymbol{w} + (\partial_{x}\bar{\boldsymbol{B}})\partial_{p}w_{0}/4.$$

The quantum nature of the system enters not only with the coherent spin dynamics, but also through the initial state  $(w_0, \boldsymbol{w})$  and via the structure of the mean-field interaction (4). Equations (7) describe the collisionless regime of weak interaction (assumed when introducing the mean-field approximation). It is opposed to the hydrodynamic regime where collisions constantly restore a local equilibrium of the momentum distribution such that the state is described by density and velocity fields depending on x only (e.g. Ref. [8]).

Initially, the system is prepared in its spin-polarized equilibrium state, with the spins pointing in x-direction, temperature T, and chemical potential  $\mu$ . One has

$$w_0(x,p) = \frac{1}{2\pi} \left\{ \exp\left[\frac{1}{T} \left(\frac{1}{2}p^2 + \frac{1}{2}x^2 - \mu\right)\right] + 1 \right\}^{-1}$$
 (8)

and  $\mathbf{w} = (1,0,0)w_0/2$  or, equivalently,  $w_{m'm} = w_0/2$ . The zero-temperature chemical potential, the Fermi energy for just one spin-state, simply reads  $E_F = N$  with total particle number  $N = \int \mathrm{d}x \, n_0(x)$ . This state is the correct equilibrium state, since the spin-polarized gas is non-interacting and the semiclassical approximation exact for a harmonic trap. Then, at time t = 0, during a preparatory pulse a z-polarized magnetic field gradient is applied. The pulse shall be short compared to other relevant time scales and is captured by  $\mathbf{B}(x) = qx\delta(t)\mathbf{e}_z$ . A spin spiral of wave length  $\lambda_s = 2\pi/q$  is created (as proposed also in Ref. [3]);  $w_0$  is still given by Eq. (8) and

$$\mathbf{w}(x,p) = (\cos(qx), \sin(qx), 0) w_0(x,p)/2, \qquad (9)$$

or  $w_{m'm}(x,p) = \exp[iqx(m-m')]w_0(x,p)/2$ . With a simple spin rotation, we have prepared a state far from thermal equilibrium. Apart from (i) having artificially created a spiral spin configuration (9) (favorable for neither energy minimization nor entropy maximization), we have also increased the number of available single-particle states from one spin state to two. The latter has two consequences: (ii) the density configuration (8) is far from being thermal (for half the number of particles per spin state having the same kinetic energy as before, a thermal distribution is characterized by a lower chemical potential and a higher temperature), and (iii) we have suddenly introduced interaction to the system. We will show in the following that the combination of (i) and (iii) leads to robust dynamical spin segregation.

When integrating the time evolution for many fermions, the semiclassical phase-space equations (7) are usually much easier to treat numerically than Eqs. (3), even though the interaction is non-local in the former,

$$V_{\rm mf}(x) = \frac{g}{2} \int \mathrm{d}p \, w_0(x, p), \quad \boldsymbol{B}_{\rm mf}(x) = -2g \int \mathrm{d}p \, \boldsymbol{w}(x, p). \tag{10}$$

This is exemplified by our state (8) and (9): In phase space, it has a linear extent  $\Delta \sim \sqrt{\max(\mu, T)}$ , we define  $\Delta \equiv 2\max(\sqrt{2N}, 2\sqrt{T})$ , while it varies on the scale

 $\delta \sim \min \left( T/\Delta, \lambda_s \right)$  stemming either from the former equilibrium or the induced spin spiral. For a reasonable phase-space representation one, thus, requires a grid of just more than  $(\Delta/\delta)^2 \sim N$  points. On the other hand, the real-space single-particle density matrix  $n_{m'm}(x',x)$  varies on the much shorter length  $\delta' \sim \Delta^{-1}$  in each argument, calling for more than  $\Delta^4 \gtrsim N^2$  grid points.

In the following we consider Li<sup>6</sup> atoms with mass  $M \approx 1.0 \cdot 10^{-26}$  kg and the scattering length tuned down to  $a_s \approx 2.4 \cdot 10^{-10} \text{m}$  by using a magnetic Feshbach resonance; the trap frequencies read  $\omega = 2\pi \cdot 60$ Hz and  $\omega_{\perp} = 2\pi \cdot 3.6$  kHz. Returning to dimensionless units, we obtain the weak coupling  $q \approx 0.055$ . The initial spin-polarized equilibrium is characterized by the particle number  $N = E_F = 100$  and by the temperature T taking values of either  $T/E_F = 0.2$ , 1, or 5 corresponding to the degenerate, intermediate and non-degenerate regime. According to these values one finds: the chemical potentials  $\mu/E_F \approx 1.0, 0.54, -7.2$ ; cloud extensions  $\Delta \approx 28, 40, 89$ ; maximum densities  $n_0(0) \approx 4.4, 3.3, 1.8$ ; and maximum mean-field potential strengths  $n_0(0)q \approx$ 0.24, 0.18, 0.097 that are small compared to the trap frequency 1 and extremely small with respect to typical single-particle energies  $\max(T, \mu) \gtrsim 100$ . In addition to temperature, we also vary the spiral wave length, taking values  $\lambda_s/\Delta = 1, 0.5, 0.2$ . For these conditions, we integrate the time evolution using a MacCormack method [9] and trust results that coincide for grid-sizes 300<sup>2</sup> and  $600^2$  for a phase space region of linear extension  $\approx 2\Delta$ .

On a short time scale  $\sim 1$ , the system evolves mainly as determined by the harmonic trapping potential. That is, neglecting interaction completely for the moment,  $(w_0(x,p), \boldsymbol{w}(x,p))$  simply rotates in phase space at constant angular velocity 1; each point of the Wigner distributions follows the classical circular orbit. This behavior can be observed clearly in the first row of Fig. 1(a) showing the evolution of  $w_x$  during half a cycle. This simple dynamics in phase space translates into a more involved evolution of the spatial polarization  $\boldsymbol{n}(x) = \int \! \mathrm{d}p \, \boldsymbol{w}(x,p)$ . Fig. 1(b) shows the averaged absolute spatial xy-polarization,  $\sigma_{xy} \equiv \frac{1}{N} \int \! \mathrm{d}x \, \sqrt{n_x^2(x) + n_y^2(x)}$ , during the first two cycles. A rapid collapse of  $\sigma_{xy}$  followed by periodic revivals can be observed, the more pronounced the shorter  $\lambda_s$ .

During a single cycle, the weak interaction causes only small deviations from a simple rotation in phase space. The small modification of the trap frequency and the slight anharmonicities caused by the scalar part of the mean-field potential  $V_{\rm mf}(x)$  are hardly noticeable. The effect of interaction becomes apparent, however, in  $w_z$ , being zero initially [Fig. 1(a), note the different color scales]. Though still small,  $w_z$  develops a characteristic pattern induced by the magnetic mean field  $\boldsymbol{B}_{\rm mf}$  stemming from exchange interaction. Namely, in  $w_z$  two domains of opposite z-polarization form. This spin segrega-

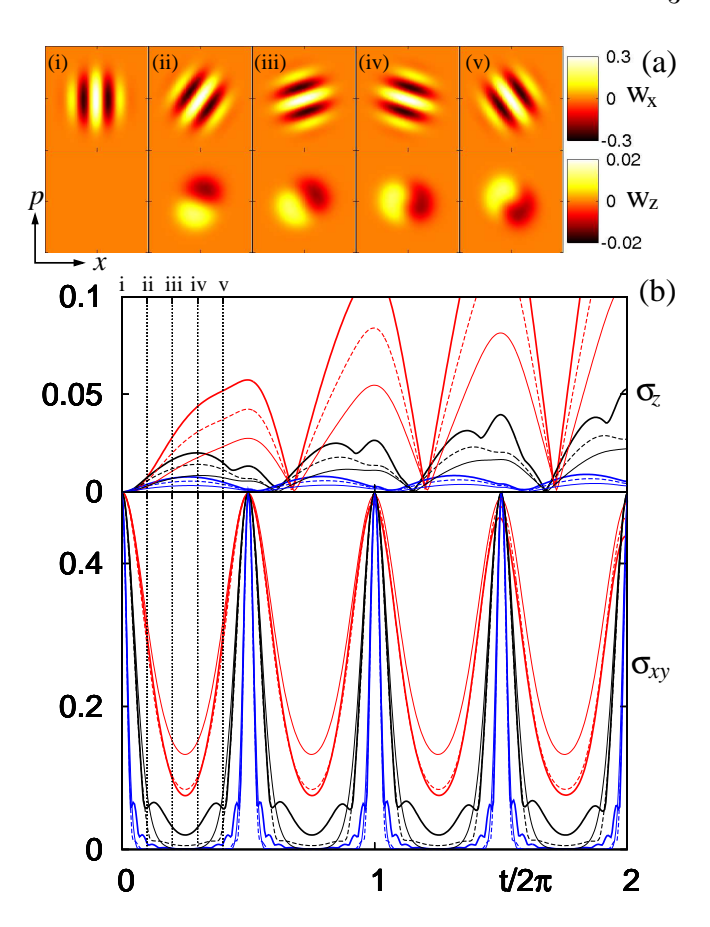


FIG. 1: (a)Wigner functions  $w_x(x,p)$  and  $w_z(x,p)$  at five times [i-v, as indicated in Fig. (b)] during the first half cycle;  $T/E_F = 1$ ,  $\lambda_s/\Delta = 2$ , and both x and p range from -40 to 40. (b) Time evolution of the polarizations  $\sigma_z$  and  $\sigma_{xy}$  for  $T/E_F = 0.2$ , 1, 5 (thick solid, dashed, and thin solid lines, respectively) and for  $\lambda_s/\Delta = 1$ , 0.5, 0.2 (upper triple of red, central triple of black, and lower triple of blue lines, respectively).

tion in phase space corresponds to phase-opposed dipole oscillations of the  $\uparrow$ - and the  $\downarrow$ -polarized domain in the trap. Remarkably, the segregation into two spin domains (and only two) is a very robust effect; we find it for all pitches of the spin spiral considered here. The upper panel of Fig 1(b) shows the averaged absolute spatial z-polarization  $\sigma_z \equiv \frac{1}{N} \int \mathrm{d}x \, \sqrt{n_z^2(x)}$ . As a consequence of spin segregation,  $\sigma_z$  oscillates in time, however, because only two domains are formed it does not feature sharp collapses like  $\sigma_{xy}$  in the case of small  $\lambda_s/\Delta$ .

In Fig 2 we present data also for longer times, for  $T/E_F = 1$  and three different spiral wave lengths  $\lambda_s/\Delta$ : From cycle to cycle the spin segregation becomes more and more pronounced as visible from  $\sigma_z$  and the snapshots on the r.h.s. showing  $w_z$  during the 21st half cycle. At the same time, the spiral spin structure in the xy-plane, visible in  $w_x$ , decreases, but stays intact. The spin segregation can directly be controlled by the number of windings of the spin spiral within the cloud, the shorter

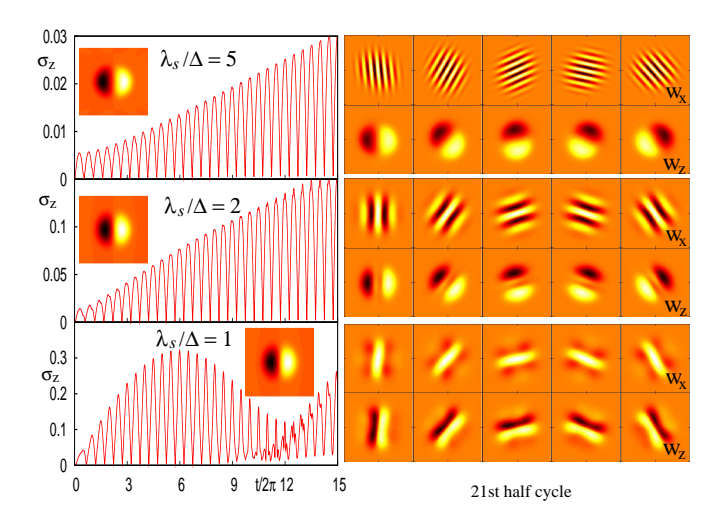


FIG. 2: Evolution for longer times,  $T/E_F = 1$ , and different wave lenghts  $\lambda_s/\Delta$ : Polarization  $\sigma_z$ ;  $[\mathbf{B}_{\mathrm{mf}}^{\mathrm{cyc}}(0) \times \mathbf{w}(0)]_z$  (insets); and Wigner functions  $w_x$  and  $w_z$  for five times like in Fig. 1(a), but during the 21st half cycle.

 $\lambda_s/\Delta$  the slower the segregation builds up. The fastest segregation is observed for  $\lambda_s/\Delta=1$ , here already after 10 half cycles deviations from a linear increase is found and a more complex dynamics sets in. While initially, the phase-space axis connecting the  $\uparrow$  and the  $\downarrow$  domain appears orthogonal to the orientation of the spin-spiral [Fig. 1(a)], after a few cycles both axes lie parallel [Fig. 2, r.h.s.]; this process can be monitored also in Fig. 1(b).

We can explain the spin segregation in a perturbative way. Observing  $(w_0, \boldsymbol{w})$  with respect to the rotating frame with coordinates  $x' = x\cos(\omega t) + p\sin(\omega t)$ and  $p' = p\cos(\omega t) - x\sin(\omega t)$ , it becomes stationary for vanishing interaction. Interaction, represented by the mean-field potentials (10), is now time-dependent, since it is obtained by projecting onto the x-axis that rotates in the new frame. Assuming that interaction causes only minor changes during a cycle, we can approximate the mean-field potentials by averaging over one cycle while keeping  $(w_0(t), \boldsymbol{w}(t))$  constant, e.g. with  $x(\tau) = x' \cos(\omega \tau) - p' \cos(\omega \tau)$  and  $p(\tau) = p' \cos(\omega \tau) + x' \sin(\omega \tau)$  [10]. The insets of Fig. 2 show  $[\boldsymbol{B}_{\mathrm{mf}}^{\mathrm{cyc}}(0) \times \boldsymbol{w}(0)]_z$ , the change rate of  $w_z$  due to coherent rotation of spins in the local cycle-averaged magnetic mean field, computed for the initial state. Notably, we always find a pattern showing two oppositely polarized domains, irrespective of the number of windings  $\Delta/\lambda_s$ (slight deviations from this behavior are found for low temperatures). This remarkable feature of  $[{m B}_{
m mf}^{
m cyc}(0)$  ×  $w(0)|_z$  is a consequence of the complex interplay between (i) the spiral structure, (ii) rotation in phase space, and (iii) the fact that interaction is non-local with respect to momentum p. It can be explained as follows. Averaged over a cycle, a spin interacts most strongly with

the mean-field created by other spins close by in phase space. Whether a spin is rotated in positive or negative z-direction is, thus, determined by the averaged polarization in its phase-space neighborhood. This averaged neighborhood polarization, in turn, is dominated by the polarization of those neighbors found when moving along the spiral towards higher spin densities, i.e. towards the origin x = p = 0. On one side of the spiral this leads always to positive, on the other side always to negative z-polarization. Moreover, the strength of the local meanfield depends on the spatial variation of the spin density compared to the spiral wave length  $\lambda_s$ ; the smaller  $\lambda_s/\Delta$ the slower the spin segregation. We have identified the mechanism underlying the observed spin segregation into two domains. Obviously, the phenomenon does not depend on the sign of the spin-spin coupling. We have checked that it is equally observable for attractive interaction. Moreover, it can also be found in a non-condensed Bose gas which is equally described by Eqs. 7, but with the exchange interaction having opposite sign.

The dynamical spin segregation predicted here is — like itinerant ferromagnetism — caused by exchange interaction. However, while the Stoner transition to a ferromagnetic phase is an equilibrium effect requiring fairly strong interaction (as well as spatial dimensionalities larger than one), the robust effect described here happens far from equilibrium and does not need strong interaction but, instead, sufficiently long times to build up. The possibility that small perturbations can lead to noticeable effects already on the mean-field level by integrating up on long times marks a fundamental difference between equilibrium and non-equilibrium many-body physics.

We acknowledge support by the Spanish MICINN (FIS 2008-00784), the A.v. Humboldt foundation, ERC Grant QUAGATUA, and EU STREP NAMEQUAM.

- \* Electronic address: andre.eckardt@icfo.es
- M. Lewenstein et al., Adv. Phys. 56, 243 (2007); I. Bloch,
   J. Dalibard, and W. Zwerger, Rev. Mod. Phys. 80, 885 (2008).
- M. Vengalattore, S. R. Leslie, J. Guzman, and D. M. Stamper-Kurn, Phys. Rev. Lett. 100, 170403 (2008); J. Kronjäger et al., Phys. Rev. Lett. 105, 090402 (2010).
- [3] G. J. Conduit and E. Altman, Phys. Rev. A 82, 043603 (2010).
- [4] X. Du, L. Luo, B. Clancy, and J. E. Thomas, Phys. Rev. Lett. 101, 150401 (2008); X. Du, Y. Zhang, J. Petricka, and J. E. Thomas, Phys. Rev. Lett. 103, 010401 (2009).
- [5] F. Pièchon, J. N. Fuchs, and F. Laloë, Phys. Rev. Lett. 102, 215301 (2009); S. Natu and E. J. Mueller, Phys. Rev. A 79, 051601(R) (2009).
- [6] G.-B. Jo, Y.-R. Lee, J.-H. Choi, C. A. Christensen, T. H. Kim, J. H. Thywissen, D. E. Pritchard, and W. Ketterle, Science 325, 1521 (2009).

- [7] G. J. Conduit and B. D. Simons, Phys. Rev. Lett. 103, 200403 (2009); A. Recati and S. Stringari, Phys. Rev. Lett. 106, 080402 (2011).
- [8] J. N. Fuchs, D. M. Gangardt, and F. Laloë, Eur. Phys. J. D 25, 57 (2003).
- [9] R. MacCormack, J. Spacecraft and Rockets 40, 757 (2003).
- [10] This approximation can be refined by applying quan-

tum Floquet theory to the many-body problem in the Dirac picture (co-rotating frame in phase space), similar as it has been done for a Wannier-Stark system, A. R. Kolovsky and A. Buchleitner, Phys. Rev. E **68**, 056213 (2003), or a driven lattice, A. Eckardt and M. Holthaus, Europhys. Lett. 80, 50004 (2007); A. Eckardt and M. Holthaus, Phys. Rev. Lett. **101**, 245302 (2008).